# Large-Scale Precursors to Major Lake Effect Snowstorms Lee of Lake Erie

Honors Research Thesis

Fall 2011-Spring 2012

17 May 2012

Hannah E. Attard and Ross A. Lazear

Department of Atmospheric and Environmental Sciences

State University of New York at Albany, SUNY

Albany, New York

## Abstract

Lake-effect snowstorms are primarily a mesoscale feature; however, major lake-effect snowstorms are linked closely to their synoptic environment. Thus, a lake-effect system which lasts for more than 24 h cannot only be explained by the boundary layer; it is also associated with the upper tropospheric flow. This research will address whether major lake-effect snow events off of Lake Erie can also be associated with large-scale planetary features several days prior to event onset. The goal is to aid in the forecast process by increasing the accuracy and lead-time of lake-effect snow forecasts.

This study includes 31 cases recorded from the National Weather Service at Buffalo's lake effect database. These 31 cases were then stratified into categories depending on its: length, the time of year, and the type of event. This categorization allowed for comparison of the state of the atmosphere in the days prior to different types of events. In order to assess the large-scale pattern, teleconnections were used as a proxy for the state of the atmosphere. For cases that lasted for greater than 42 hours, there was a correlation to the phase Madden Julian oscillation eight days prior to onset. The cases that occurred during the positive and negative states of the Arctic Oscillation had two different upper level trough patterns, the former originating in Southern Canada and the latter over the Southwestern United States.

## 1. Introduction

Lake-effect snow is an important boundary layer feature in western New York. The formation of lake-effect snow is dependent on a cold airmass picking up heat and moisture as it flows over the warmer lakes, thereby inducing an unstable atmosphere through the transfer of energy and producing snow offshore of the lakes (Dewey, 1979). This phenomenon may occur downwind of any of the Great Lakes, but this study will focus on snowfall lee of Lake Erie.

Many studies have been conducted regarding both the meso- and synoptic-scale environments surrounding lake effect systems (e.g. Leathers and Ellis 1996, Peace 1966). This study, however, aims to focus on the large scale -- specifically the Northern Hemispheric circulation occurring in the days prior to these lake-effect systems. By studying the large-scale circulation, the goal is to identify dominant patterns in the days prior to major lake-effect events in order to aid the forecast process by increasing the lead-time and accuracy of lake-effect snow forecasts.

There are certain modes of variability which dominate the global flow pattern. These flow regimes have been characterized into indices in order to more easily assess the state of the atmosphere. The different state of the indices (usually positive or negative) explains the basic overall flow pattern of the globe. These indices will be utilized in order to quantify the state of the atmosphere and the correlation between large-scale patterns and lake effect snowstorms in the Buffalo, NY area.

The Pacific/North American Pattern (PNA) measures the amplification or dampening of the broad ridge-trough pattern across the United States (Notaro et al. 2006). Figure 1, courtesy of Leathers et al. (1991) is a schematic that displays the 700-hPa flow during both the positive and negative states of the PNA. The negative phase of the PNA is characterized by a zonal flow across the United States, whereas the positive phase is characterized by a more meridional flow, with a 700-hPa ridge over the western United States and a trough over the central and eastern United States (Leathers et al. 1991). Although these different flow regimes are apparent throughout the year, they are most highly amplified in the winter months (Leathers et al. 1991). Peace (1966) concluded that the surface conditions associated with lake-effect snow such as land breeze, shoreline frictional convergence, and orographic effects are not the primary cause of lake effect snow, but rather a response to the upper levels that drive these systems. With this in mind it was hypothesized that more lake-effect events would occur during the positive state of the PNA due to the more highly amplified flow and the tendency for stronger cold air outbreaks in the northeast United States (Leathers et al. 1991).

Another commonly studied mode of Northern Hemispheric variability is the Arctic Oscillation (AO). The AO is defined as a more global pressure characteristic of the North Atlantic Oscillation (NAO), which focuses on the North Atlantic (Barry and Chorley 2010). As shown in Figure 2 (from Wallace and Gutzler 1980), the positive state of the NAO is defined as an anomalously strong Icelandic low, strong westerlies over the Atlantic Ocean, and an anomalously warm northeast United States. The negative state of the NAO is characterized by the opposite phenomena:

an anomalously weak Icelandic low, reduced westerlies over the Atlantic Ocean, and an anomalously cold northeast United States (Wallace and Gutzler, 1980). Because an important ingredient for producing lake-effect snow is a cold lower tropospheric airmass, it was expected that lake-effect events would be favored when the atmosphere is characterized by the negative phase of the NAO and thus, the negative phase of the AO.

Finally, the state of the Madden-Julian Oscillation (MJO) was also analyzed. The MJO is identified by an eastward moving pulse of convection at the equator which originates in the Indian Ocean and travels to the Western Hemisphere on 30-60 day timescales (Madden and Julian 1971). Wheeler and Hendin (2004) stratified the location of the MJO convection into eight phases. The first begins in the Indian Ocean (phase 1) and continues eastward to the Northern Hemisphere (phase 8). This anomalous convection not only influences tropical weather patterns, but also impacts the multitudes and has a notable effect on the state of the AO (L'Heureux and Higgins 2007). How this, in turn, affects lake-effect snow in Buffalo, NY is analyzed in this paper.

## 2. Data and Methodology

### *a. Methodology*

The initial case list for this study was recorded from the National Weather Service at Buffalo's (NWS Buffalo) lake effect database, in which cases are named and recorded from 1998 to the current season. The criteria for a storm to be named includes the following: at least 17 cm of snowfall in 24 h, the snow to be all or primarily lake effect, and for it to occur in the County Warning Area (CWA) (S.

McLaughlin 2011, personal communication). As this study focuses on "major" lake-effect snowstorms off of Lake Erie, these criteria were refined. In order for a storm to be included in this study it must have produced at least 30 cm in 24 h, occurred off of Lake Erie, and not include snowfall totals from a synoptic system or lake-enhanced snowfall. As shown in Figure 3, the Buffalo CWA incorporates both Lakes Erie and Ontario, which are significant lake-effect snow producers. For the purpose of this study, the focus will be on Lake Erie, meaning any named cases on the Buffalo Lake Effect page that have snowfall maxima from Lake Ontario were discounted.

Of the 137 named lake-effect storms in the Buffalo CWA, 62 fit the criteria of a "major" storm. However, some of these named storms include both lake-enhanced and lake-effect snowfall totals. To ensure that the cases in the study were purely lake effect, radar data from the National Climatic Data Center (NCDC) was analyzed. Figure 4 is a radar example of both an accepted and a rejected case. The first image, Figure 4a, depicts a classic shore parallel lake-effect snow band and one which was used in this study. Figure 4b, however, displays that the snow in this case began with a synoptic-scale system and the total amount of snow included lake-enhanced amounts. The case list was reduced to 52 cases that were deemed to be purely lake-effect systems. The NCDC radar data was also utilized to determine the start and end times of each case to the nearest six-hour interval (0000 UTC, 0600 UTC, 1200 UTC, 1800 UTC).

Finally, the case list was also refined by rejecting any snowstorm that occurred within seven days after the previous case ended because the resultant mean flow would not necessarily be representative of the flow in the days prior to

major events. With these criteria, the final number of cases for this study was 31. Although this is not enough cases to make a statistically significant conclusion, it is a preliminary study of large-scale precursors to lake-effect snowstorms. In order to draw definite conclusions a larger case list is necessary.

Once the final case list was determined, the 31 cases were stratified into three category types (Table 1). These categories were created to facilitate comparisons of the large-scale patterns in the days prior to each type of case. The storm length of 42 h was arbitrarily chosen to split the cases as evenly as possible. Also the cases that last for over 42 h are likely associated with a less transient large-scale pattern. Lake-effect systems are usually shorter in duration; therefore, there were a smaller number of cases that lasted for over 42 h. In regards to the split between earlier and late season cases, for the later season cases (JFMA) the lake is cold from the winter, thus for lake-effect snow to develop, there must be a significantly cold 850-hPa airmass. However, for the earlier season cases (OND), the lake is warmer, so the 850-hPa airmass does not need to be as cold as the later season cases to produce snow. Lastly, the dichotomy between the different dominant lake-effect bad types consists of 24 shore parallel cases and 7 wind parallel cases. This uneven divide is due in part to the nature of these systms. Shore parallel systems tend to produce more snowfall due to the longer fetch over the lake whereas wind parallel systems are less organized and more variable (Dewey, 1979).

*b. Data*

Climate Forecast System Reanalysis (CFSR) (0.5° data) was utilized for this study. Composite maps were made for each of the previously described categories

from 14 days prior to onset to event onset. Standardized anomalies were also computed using the NCEP/NCAR Reanalysis dataset (2.5° x 2.5° resolution) with climatology of 1979-2008.

## 3. Results

The results section will be divided into discussions of each teleconnection pattern and its subsequent potential correlations between lake effect systems in the Buffalo, NY area. Each of the case categories were analyzed except for the type of band organization (shore parallel and wind parallel), as it would not be valid to make such comparisons given the unequal number of cases in each category. Although each case category was analyzed, significant results were not found in all of the categories, and this will also be addressed.

### *a. MJO signal*

This section will focus on the cases that lasted for longer than 42 h. Figure 5 is the composite 500-hPa height and standardized anomalies eight days prior to onset for the cases that lasted greater than or equal to 42 h. Over the western Pacific is a +1 standard deviation 500-hPa height anomaly. To ensure that this was not a manifestation of one or two strongly positive height anomalies, a spaghetti plot of the 576 dam contour was created (Figure 6). Each of the 11 cases is plotted along with the mean height. Over the western Pacific, there is very small spread among all of the cases whereas throughout the rest of the hemisphere there is significant spread. A certain amount of this small spread may be attributed to the strong height gradient in this area, although there is also a strong gradient over the Atlantic Ocean, where the spaghetti plot indicates a large spread among all of the

cases. Therefore, the +1 standard deviation over the Western Pacific seems to be significant and representative of all eleven cases.

Figure 7 (from Climate Prediction Center) shows a schematic of convection occurring at the equator and the midlatitude response. As shown, the upper atmosphere is associated with anticyclonic circulation in the midlatitudes associated with the equatorial convection. This is due to latent heating and increased thickness both to the north and south of the convection. In order to determine if this is the cause of the aforementioned 500-hPa positive height anomalies for cases that lasted for longer than 42 h eight days prior to the onset of lake effect snow in Buffalo, NY, composite mean and anomaly outgoing longwave radiation (OLR) values were plotted using the Earth System Research Laboratory (ESRL). Figure 8a shows the composite mean values of OLR eight days prior to onset. The lowest values of 180 $Wm^{-2}$ are located over Papua New Guinea indicating deep convection in this area. In order to determine if this is anomalous convection, Figure 4b displays the OLR anomalies at this time. The -30 $Wm^{-2}$ anomaly collocated in the area of deep convection suggests that this is anomalous convection.

In order to determine if this anomalous tropical convection has a connection to the MJO, the phase of the MJO for each of the 11 cases eight days prior to onset were plotted on an MJO phase space diagram (Figure 9). As is evident in this figure there is a clustering of cases that occurred when the MJO was in phases six and seven (convection in the Western Hemisphere) eight days prior to onset. This is the same location where the OLR values (Figure 8) indicate anomalous convection

occurring. Therefore, it seems as though the convection over Papua New Guinea eight days prior to onset is associated with MJO convection.

The connection between the MJO and lake-effect systems is apparent through the connection between the MJO and the state of the AO as shown by L'Heureux and Higgins (2007). L'Heureux and Higgins (2007) concluded that the AO favors a negative tendency when the MJO is in phases six and seven. Figure 10 (courtesy of L'Heureux and Higgins, 2007) is a graphical representation of this conclusion and clearly shows the negative tendency of the AO during MJO phases six and seven. The negative phase of the AO is characterized by positive height anomalies in the high latitudes and cold temperature anomalies in the northeast United States (Wallace and Gutlzer 1980). Figures 11a and 11b are schematics displaying these phenomena. Comparing the positive and negative states of the AO, it would be expected that more lake-effect snow outbreaks would occur during the negative state due to the colder air outbreaks and the more meridional flow.

Not only does MJO convection influence the state of the AO, L'Heureux and Higgins (2007) also concluded that when in phases seven and eight, the MJO itself influences the midlatitude temperature and height anomalies in a way that resembles the negative phase of the AO, although smaller in amplitude.

*b. AO-relative composites*

For the purpose of this section, the state of the AO was recorded at onset. Interestingly, of the 31 cases, 15 occurred during the positive phase of the AO and 16 during the negative phase. This fairly even split between cases occurring in the positive versus negative phases of the AO was unexpected. The initial hypothesis

was that major lake effect events would occur during the negative phase of the AO when there are cold temperature anomalies in the northeast United States a more meridional flow pattern across the Northern Hemisphere.

Figure 12 shows the 500-hPa mean height at onset for the cases that occurred in the positive and negative phase of the AO. The maps are similar, however there is a noticeable difference in the ridge over the western United States. As expected, cases which have a negative phase of the AO at onset (Figure 12b) show a much more highly amplified ridge over the western United States, which reaches to the north of Alaska. The upstream ridge for the cases that occurred during the positive phase of the AO (Figure 12a), however, is much broader and less amplified, only reaching into Northern Canada.

Three days prior to lake effect onset, there are very obvious differences in the planetary flow at 500 hPa. Figure 13 shows the composite of the cases that occurred during the positive phase of the AO and the associated anomalies. Three days prior to onset (Figure 13a), there is a broad trough over southern Canada with an associated upstream ridge. There is also a trough equatorward of this ridge, which is enhancing a blocking pattern in the Pacific and leading to the deepening of the downstream trough. The east Pacific ridge three days prior to event onset is associated with a +150 m 500-hPa height anomaly (Figure 13b). Continuing in time, Figures 13c and 13d are the associated mean and anomalies, respectively, at two days prior to onset. The Pacific ridge continues to amplify, but remain stationary. The deepening of the downstream trough over Northern Canada is apparent one day prior to onset (Figure 13e), as a response to the amplified upstream ridge.

Finally, as mentioned previously, at onset there is trough over the great lakes region associated with a -150 m 500-hPa height anomaly (Figure 13g).

Despite it being in the same location and of the same anomaly, the origin of the great lakes trough for the cases that occurred during the negative phase of the AO is very different from those occurring during the positive phase of the AO. Figure 14a shows the composite mean of the 500-hPa height three days prior to onset for the negative state of the AO cases. As would be expected, during the negative state of the AO, the flow is much more meridional. There is a highly amplified ridge in the eastern Pacific that extends into Alaska and a downstream trough over California. There is also a trough extending from the high latitudes into Canada and the northeast United States. The negative AO composite anomaly pattern three days prior to onset is markedly different than the positive AO composite (Figures 14a,b). There is a +90 m 500-hPa height anomaly over Alaska and a -60 m height anomaly over southern California and the northeast United States. The northeast United States is already showing negative height anomalies in the region that the lake effect snow will occur, and the trough that will be associated with the lake effect snow is now originating in California as opposed to Canada. Moving forward in time, at two days prior to onset (Figure 14c), the trough over the southwestern United States begins to move to the northeast and starts to merge with the western edge of the eastern Canadian trough as the ridge over Alaska continues to build. One day prior to onset (Figure 14e), the upstream ridge likely influences the deepening of the downstream trough, which is beginning to extend

into the great lakes region. At onset, the trough has extended into the region and is again anomalous by -150 m (Figure 14g).

Although the synoptic pattern is similar *at* onset between the cases that occur during the positive and negative state of the AO, with a deep trough in the great lakes region, the large-scale patterns in the days prior are vastly different.

*c. PNA influences*

Thus far, only a preliminary look at the PNA has been undertaken. It seems as though the PNA does not play a significant role in the formation of lake-effect systems in the Buffalo area. As the PNA is the dominant mode of variability in the flow at 700-hPa for the United States in the winter (Leathers et al. 1991) it was assumed this would have the most significant association with lake-effect systems. However, when stratifying the data, only nine cases occurred during the positive state of the PNA, five during the negative state, and 17 when the atmosphere was in the neutral state, herein defined as within +/- 0.5 standard deviations. This indicates that the state of the PNA appears to have little influence on the formation of major lake-effect snowstorms in the Buffalo area. A further analysis must be conducted in order to verify this statement, but so far these results are consistent with other studies such as Assel (1992), which also concluded that there was not a significant connection between the PNA and lake-effect snowfall.

**4. Conclusion**

There seems to be multiple important planetary scale precursors to major lake effect systems in the Buffalo, NY area. Eight days prior to onset of lake-effect storms, there is an MJO signal in the Western Pacific for the cases that last longer

than 42 h. Focusing on the AO, there are two different storm tracks that are favored depending on if the atmosphere is in the positive or negative state. For the positive phase, the upper level trough originates over Canada whereas during the negative phase the trough originates in the southwestern United States. The PNA, however does not seem to have a high correlation with lake effect systems.

Because there are a small number of cases in this study a definite conclusion cannot be stated at this time. In the future, a broader case list is necessary in order to perform statistical significance testing and finalize these conclusions. However, this analysis provides important groundwork for the potential forecasting implications of large-scale precursors to lake-effect snowstorms in the Buffalo, NY area.

**Acknowledgements**

I would like to thank Ross Lazear for all of his help in completing this research project. From his guidance in GEMPAK to supporting all of my research interests I could not have completed this without his help. I would also like to thank Dr. Jason Cordeira, Chris Castellano, and Kyle Griffin for providing shell scripts that were essential to completing this research in a timely manner. Also, my fellow classmates who sat with me in the maproom for hours on end, I cannot thank you enough for helping me through many a small crisis. And lastly, I would like to thank Dan Panzarella, for his help retouching many of the figures.

**References**

Assel, R.A., 1992: Great Lakes winter-weather 700-hPa PNA teleconnections. *Mon. Wea. Rev.*, **120**, 2156-2163.

Australian Government Bureau of Meteorology, cited 2012: Madden-Julian Oscillation. [Available online at http://www.bom.gov.au/climate/mjo/.]

Barry, R.G. and R.J. Chorley, 2010: *Atmosphere, Weather and Climate*. 9. Routledge, 516.

Dewey, K.F., 1979: Lake Erie Induced Mesosystems – An Operational Forecast Model. *Mon. Wea. Rev.,* **107,** 421-425.

Earth System Research Laboratory, cited 2011: Daily Mean Composites. [Available online at http://www.esrl.noaa.gov/psd/data/composites/day/.]

Gottschalk, J., V. Kousky. W. Higgins, M. L'Heureux. Madden-Julian Oscillation. [Available online at: http://www.cpc.ncep.noaa.gov/products/precip/CWlink/MJO/MJO_summary.pdf.signal was observed]

Higgins, R.W., Y. Zhou and H.-K. Kim, 2001: Relationships between El Niño-Southern Oscillation and the Arctic Oscillation: A Climate-Weather Link. *NCEP/Climate Prediction Center ATLAS 8.*

Leathers, D.J., B. Yarnal, M.A. Palecki, 1991: The Pacific/North American teleconnection pattern and United States Climate. Part I: regional temperature and precipitation Associations. *J. Climate*, **4**, 517-528.

—, and A.W. Ellis, 1996: Synoptic mechanisms associated with snowfall increases to the lee of Lakes Erie and Ontario. *International Journal of Climatology,* **10**, 1117-1135.

L'Heureux, M. L. and R. W. Higgins, 2007: Boreal winter links between the Madden-Julian Oscillation and the Arctic Oscillation. *J. Climate* **21,** 3040-3050

Madden, R.A., and P.R. Julian, 1971: Detection of a 40-50 day oscillation in the zonal wind in the tropical Pacific. *J. Atmos. Sci.*, **28**, 702-708.

National Weather Service Forecast Office Buffalo New York, cited 2006: NWS Buffalo Lake Effect Page. [Available online at http://www.erh.noaa.gov/buf/lakepage.php.]

Peace, R.L., and R.B. Sykes, 1966: Mesoscale study of a lake effect snowstorm. *Mon. Wea. Rev.*, **94**, 495-507.

Colorodo State Univeristy, cited, 2011: Virtual Institute for Satellite Integration Training. [Available online at http://rammb.cira.colostate.edu/visit/les/buf_cwa.asp]

Wallace, J.M., and D.S. Gutzler, 1980: Teleconnections in the geopotential height field during the Northern Hemisphere winter. *Mon. Wea. Rev.*, **109**, 784-812.

Wheeler, M.C., and H. H. Hendon, 2004: An All-Season Real-Time Multivariate MJO Index: Development of and Index for Monitoring and Prediction. *Mon. Wea. Rev*., **132,** 1917-1932.

## List of Tables



## List of Figures

*Figure 5:* 500 hPa height (dam) and standardized anomaly eight days prior to onset for the cases that lasted ≥ 42 h

*Figure 6*: 500 hPa spaghetti plot of 576 dam contour eight days prior to onset for the 11 cases that lasted ≥ 42 h

*Figure 7*: Schematic showing the associated midlatitude response to convection occurring at the equator. Image courtesy of Climate Prediction Center.

*Figure 8*: OLR values 8 days prior to onset for the cases that lasted ≥42 h (a) composite mean and (b) anomalies. Maps made in ESRL.

*Figure 9:* MJO phase space 8 days prior to onset for the cases that lasted ≥42 h. Phase space from The Bureau of Australian Meteorology.

*Figure 10:* MJO Phase vs. AO tendency bar graph. Image from L'Heureux and Higgins (2007).

*Figure 11:* Images describing the anomalies associated with +/-AO (a) the 500-hPa height (m) mean and anomaly and (b) Temperature anomaly in the United States Image courtesy of Higgins et al. (2001).

*Figure 12a:* 500-hPa height (m) composite mean for the cases that occurred during the (a) +AO and (b) -AO. Map made in ESRL.

*Figure 13:* Composites for the 500-hPa composite mean height (m) and anomaly (m) during the positive state of the AO: composite mean 3 days prior to onset (a), anomaly 3 days prior to onset (b), mean 2 days prior to onset (c), anomaly 2 days prior to onset (d), mean 1 day prior to onset (e), anomaly 1 day prior to onset (f), mean at onset (g), at onset anomaly (h).

*Figure 14:* Composites for the 500-hPa composite mean height (m) and anomaly (m) during the negative state of the AO: composite mean 3 days prior to onset (a), anomaly 3 days prior to onset (b), mean 2 days prior to onset (c), anomaly 2 days prior to onset (d), mean 1 day prior to onset (e), anomaly 1 day prior to onset (f), mean at onset (g), at onset anomaly (h).

**Tables**

| Case Categories | Number of Cases |
|---|---|
| All Cases | 31 |
| 24-42 h<br>≥42 | 20<br>11 |
| January, February, March, April<br>October, November, December | 15<br>16 |
| Shore Parallel<br>Wind Parallel | 24<br>7 |

**Table 1.** The stratification of the different case categories in this study and the number of cases in each category.

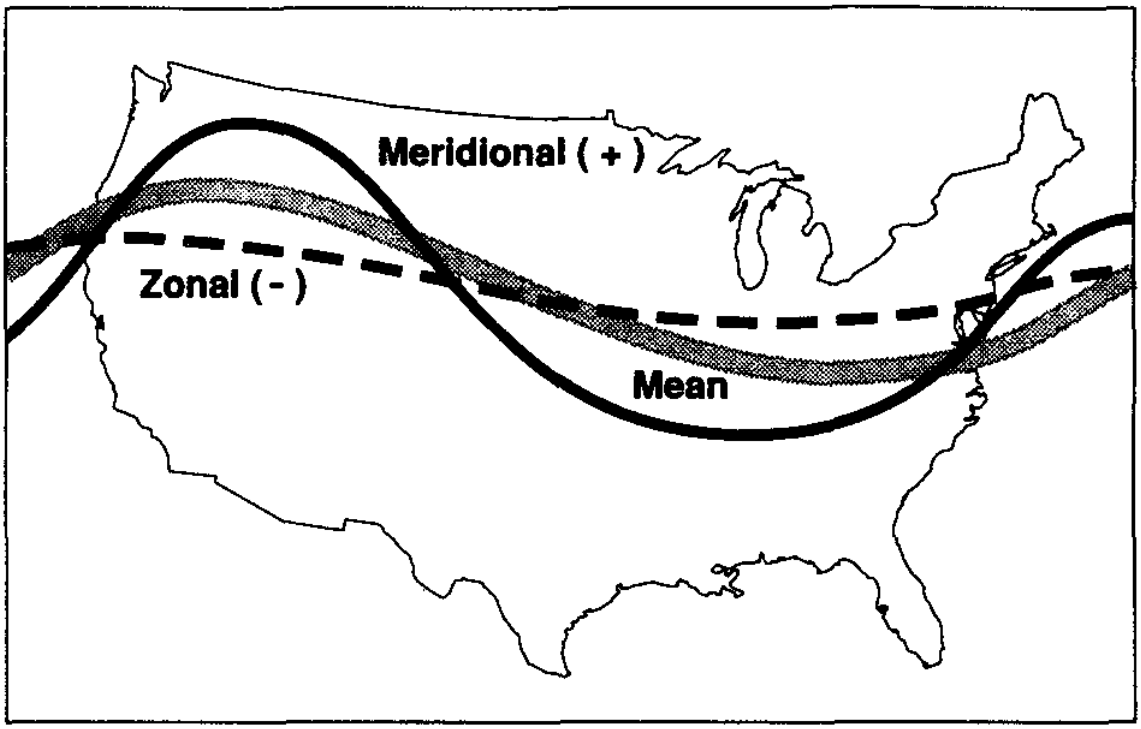


**Figure 1.** Schematic of the mean 700-hPa flow over the continental United Sates during the positive and negative states of the PNA. Image from Leather, et al. (1991)

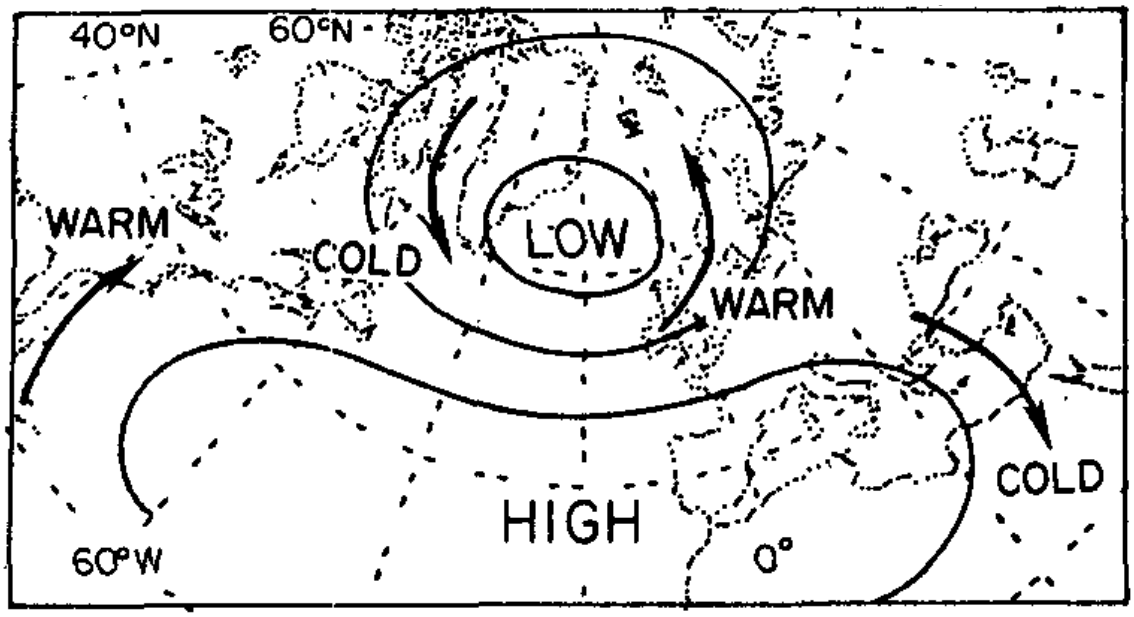


**Figure 2.** Schematic describing idealized pressure and temperature anomalies associated with the AO. Image from Wallace and Gutzler (1980).

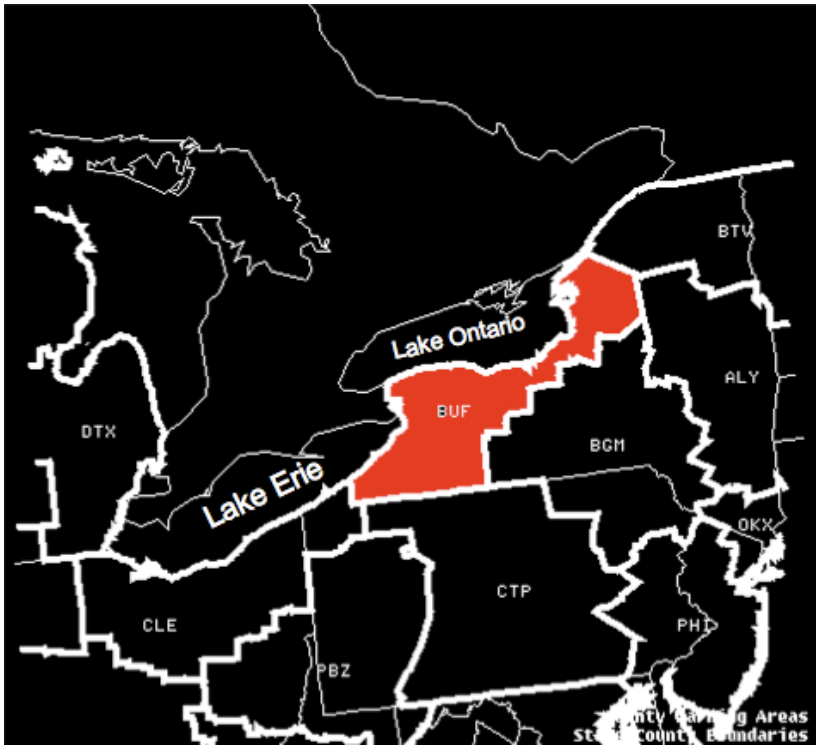


**Figure 3.** Buffalo County Warning Area. Map courtesy of Colorado State University.

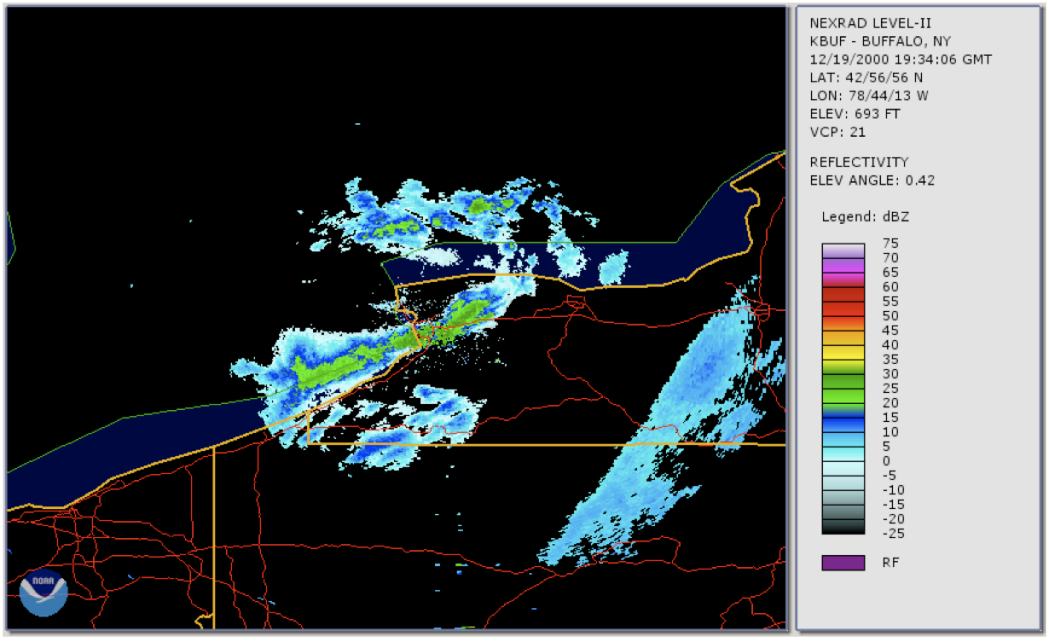


**Figure 4a.** Example of a pure lake-effect case. Image from 1934 UTC 19 December 2000. Courtesy of NCDC.

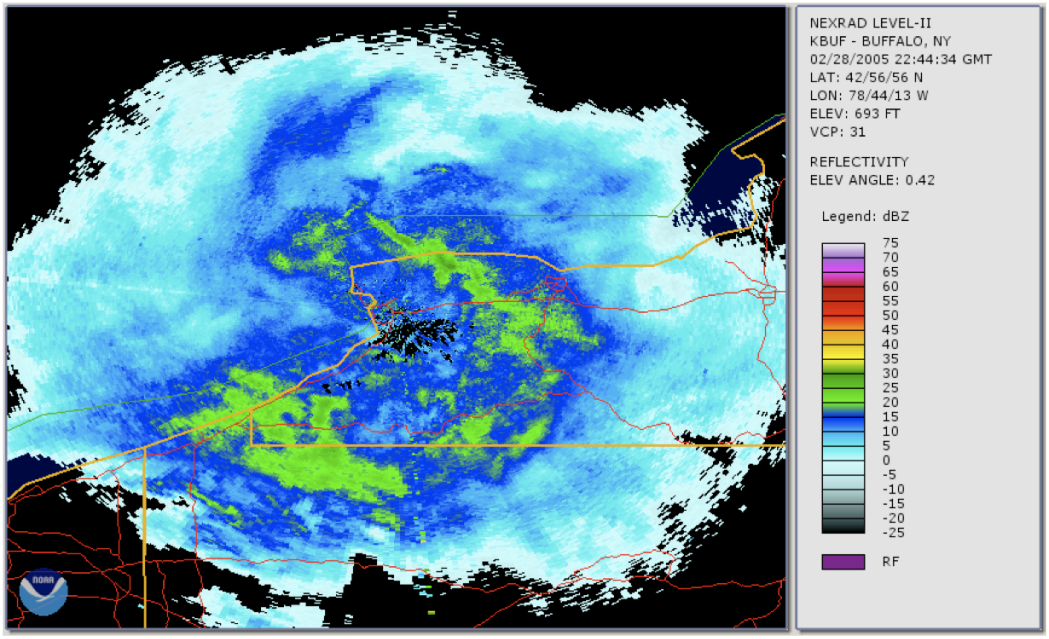


**Figure 4b.** Example of a lake-enhanced radar case. Image from 2244 UTC 28 February 2005. Image courtesy of NCDC.

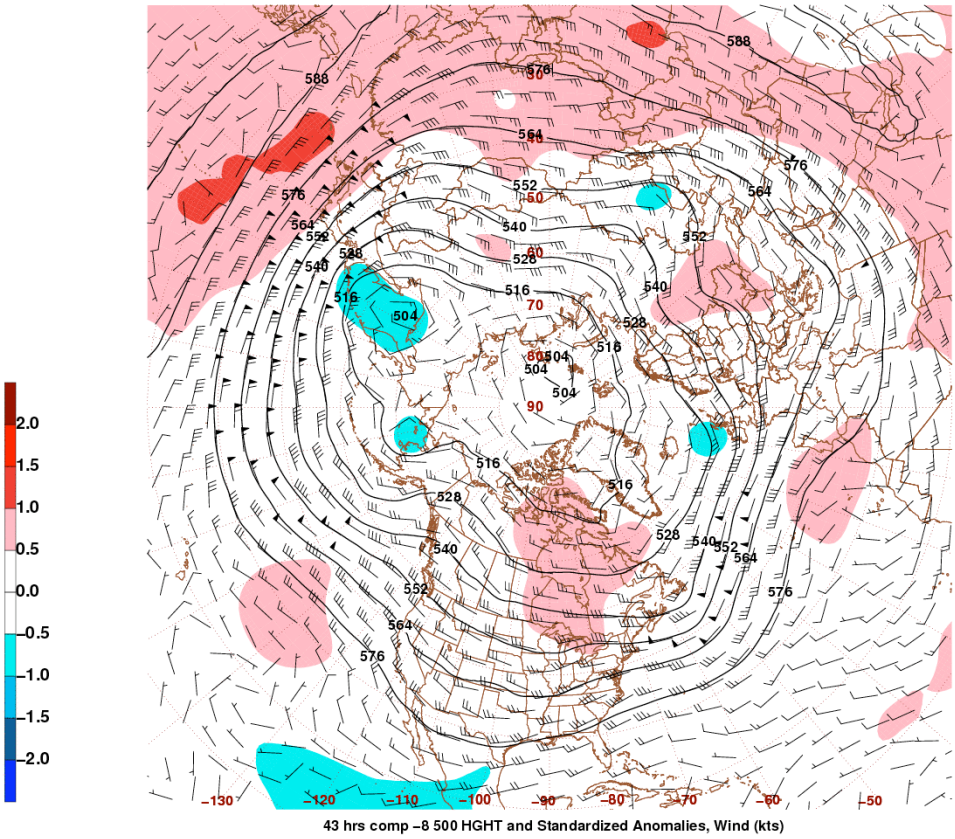


**Figure 5.** Composite of cases that lasted ≥42 h 8 days prior to onset. 500-hPa mean height (dam), wind (kts), and standardized anomalies.

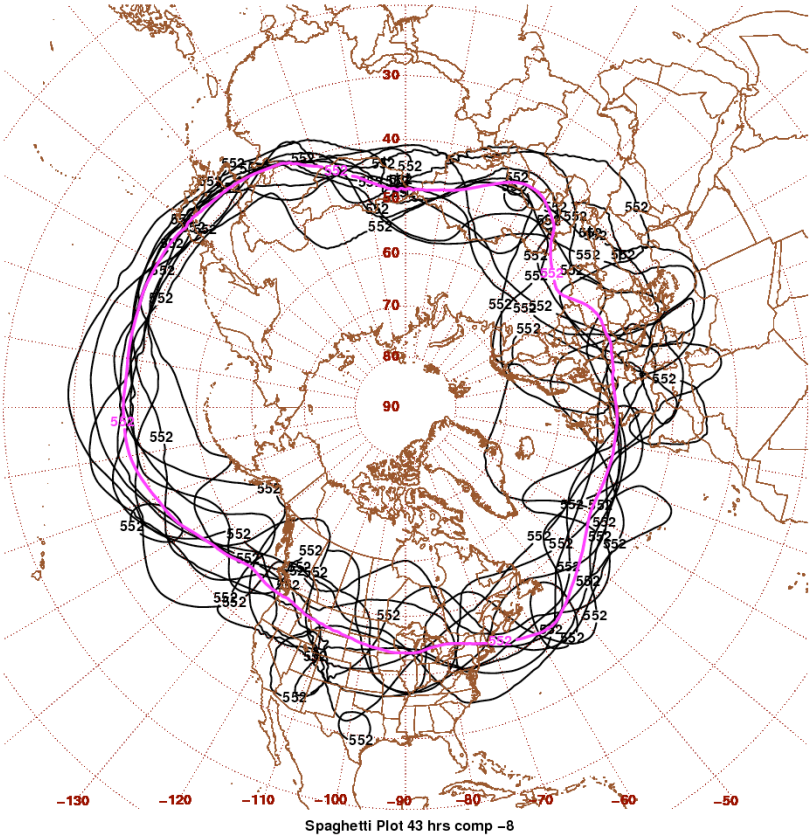


**Figure 6.** Spaghetti plot of 576 dam height contour for cases that lasted ≥42 h 8 days prior to onset. Each of the 11 cases are contoured in black and the mean is in purple.

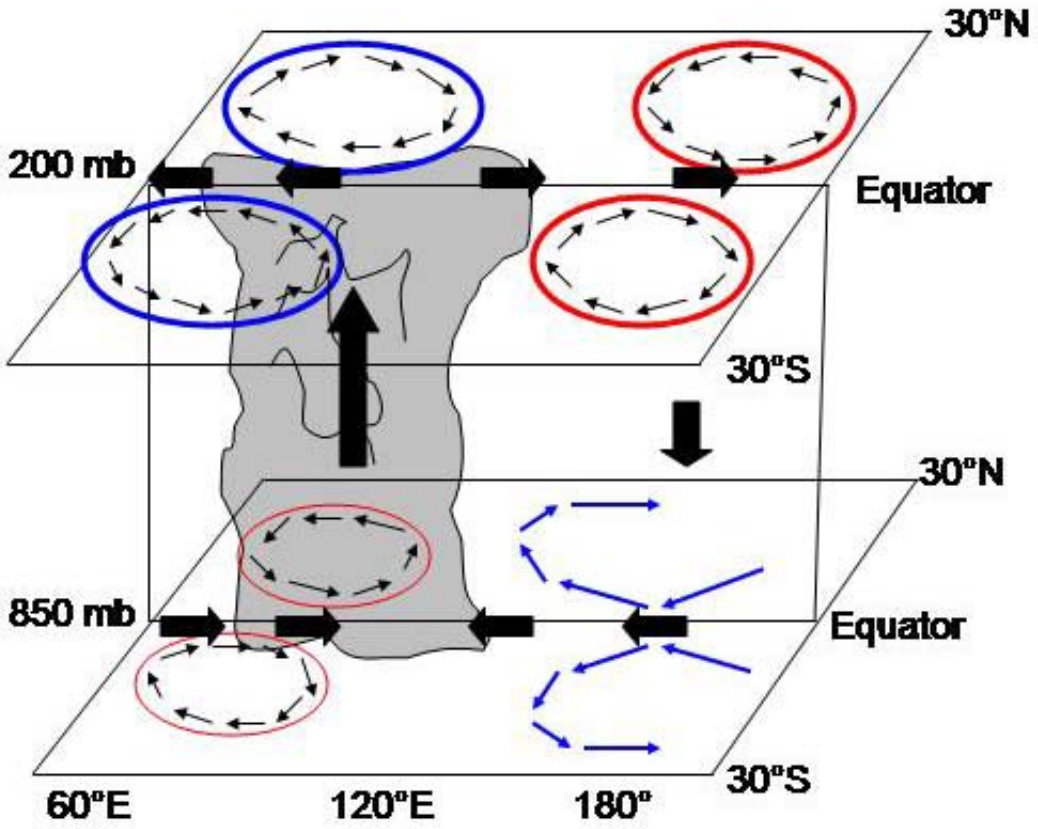


**Figure 7.** Schemetic describing circulations associated with the MJO convection. The grey plume indicates the convection, the red (blue) circles represent anticyclonic (cyclonic) circulation, the black arrows describe the wind direction and rising (sinking) motion. Image from Gottschalk et al.

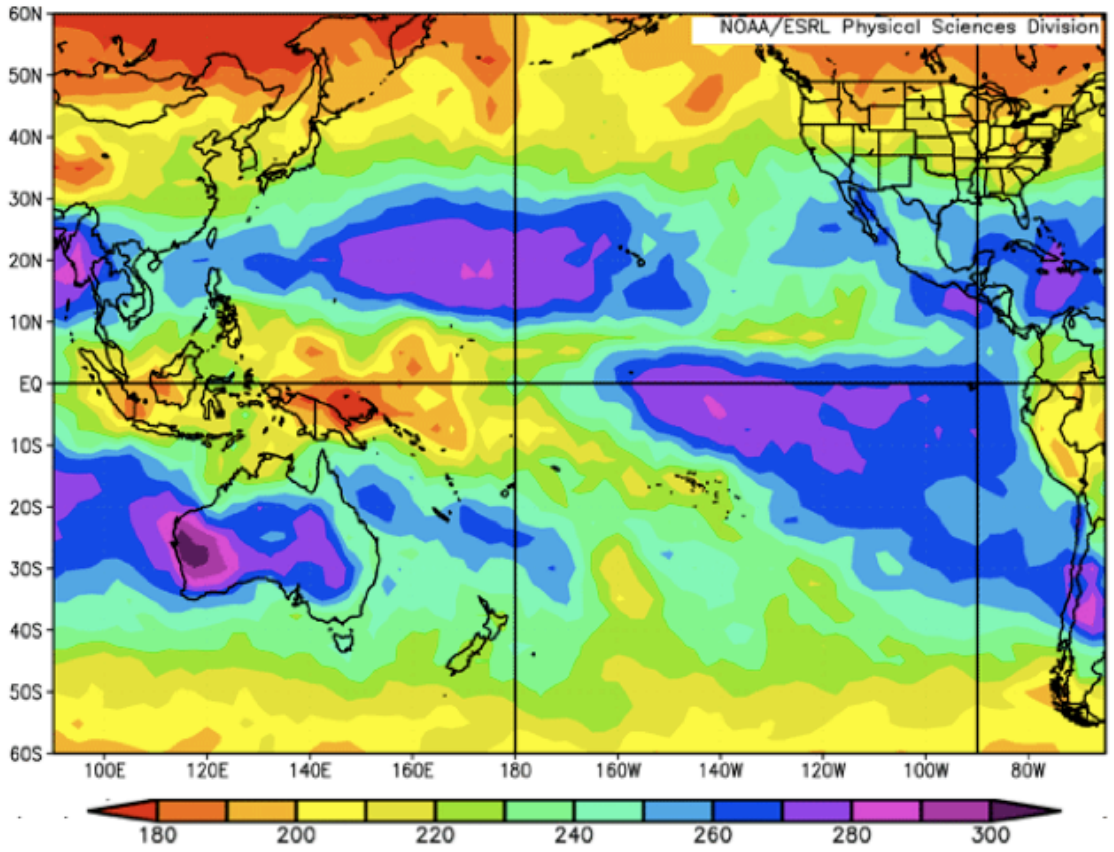


**Figure 8a.** Composite of cases that lasted ≥42 h 8 days prior to onset. Mean OLR ($W/m^2$) values. Image made in ESRL.

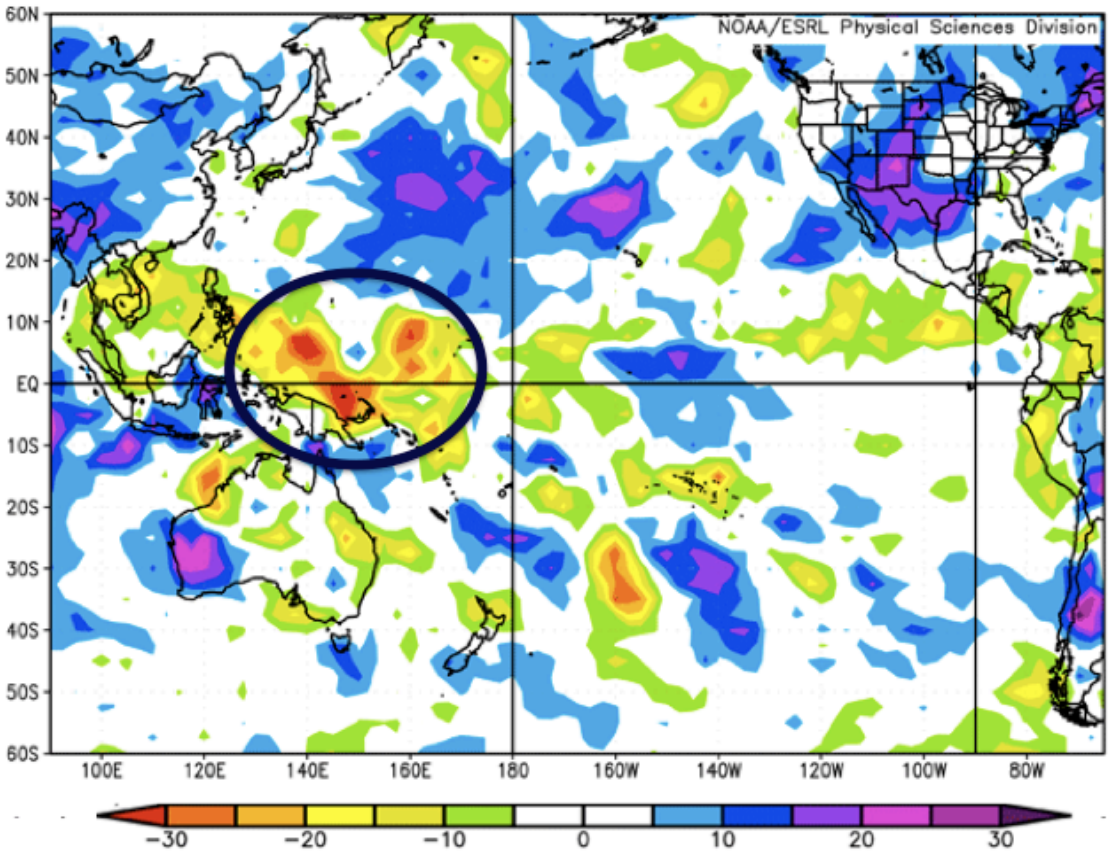


**Figure 8b.** As in 8a but anomaly OLR ($Wm^{-2}$) values. The black circle indicates the region of significant OLR anomalies. Image made in ESRL.

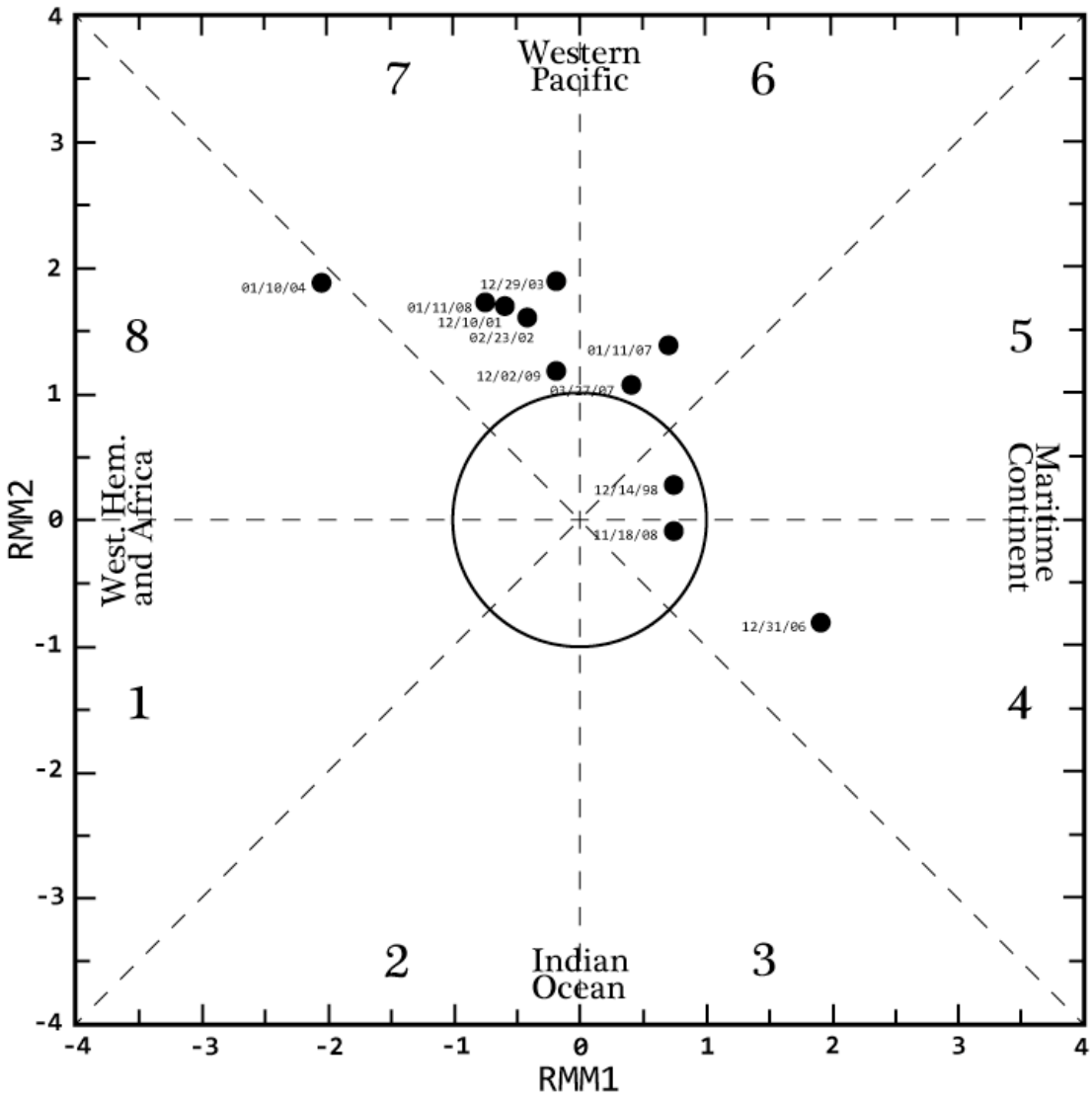


**Figure 9.** MJO phase space of cases that lasted ≥42 h 8 days prior to onset. Cases are plotted based on the phase of the MJO 8 days prior to onset. MJO Phase space from Bureau of Australian Meteorology.

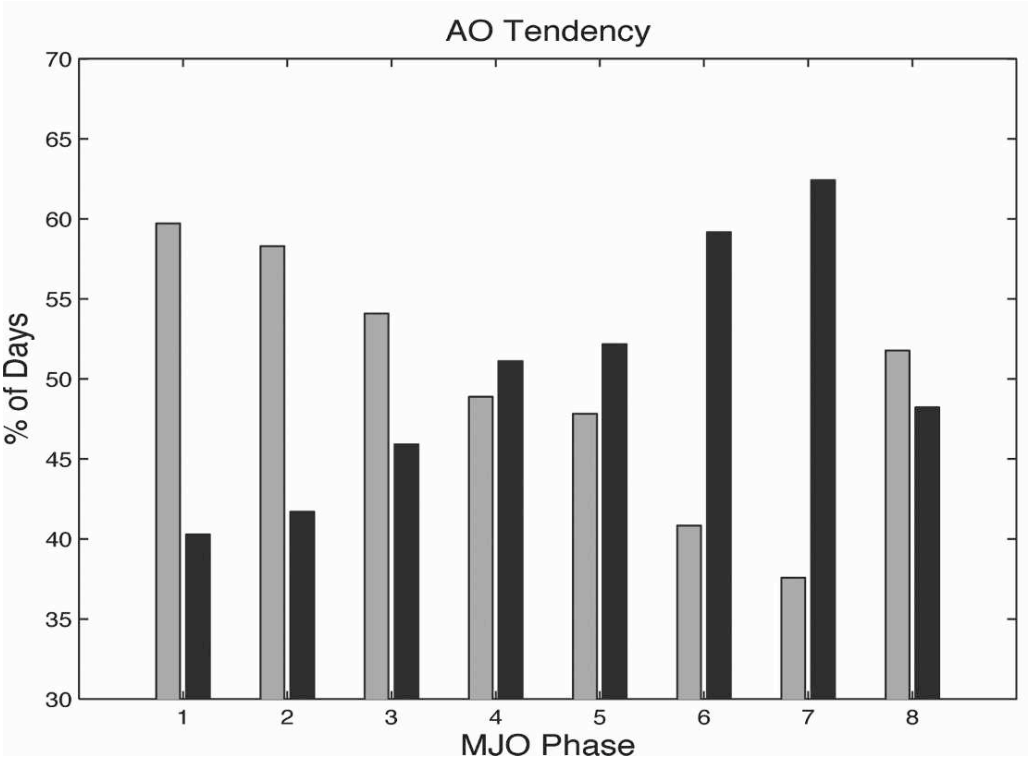


**Figure 10.** Percentage of cases when the tendency of the AO anomaly is positive (grey) vs. negative (black). Image from L'Heureux and Higgins (2007).

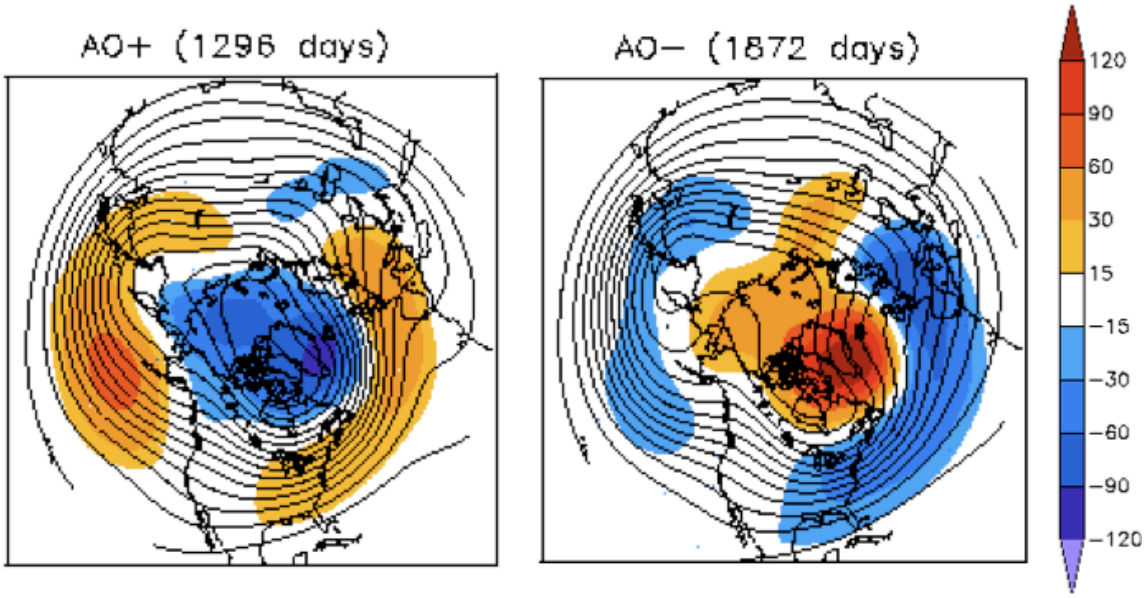


**Figure 11a**. The mean 500 hPa height and anomaly (m) during the positive and negative state of the AO. Image courtesy of Higgins et al. 2001.

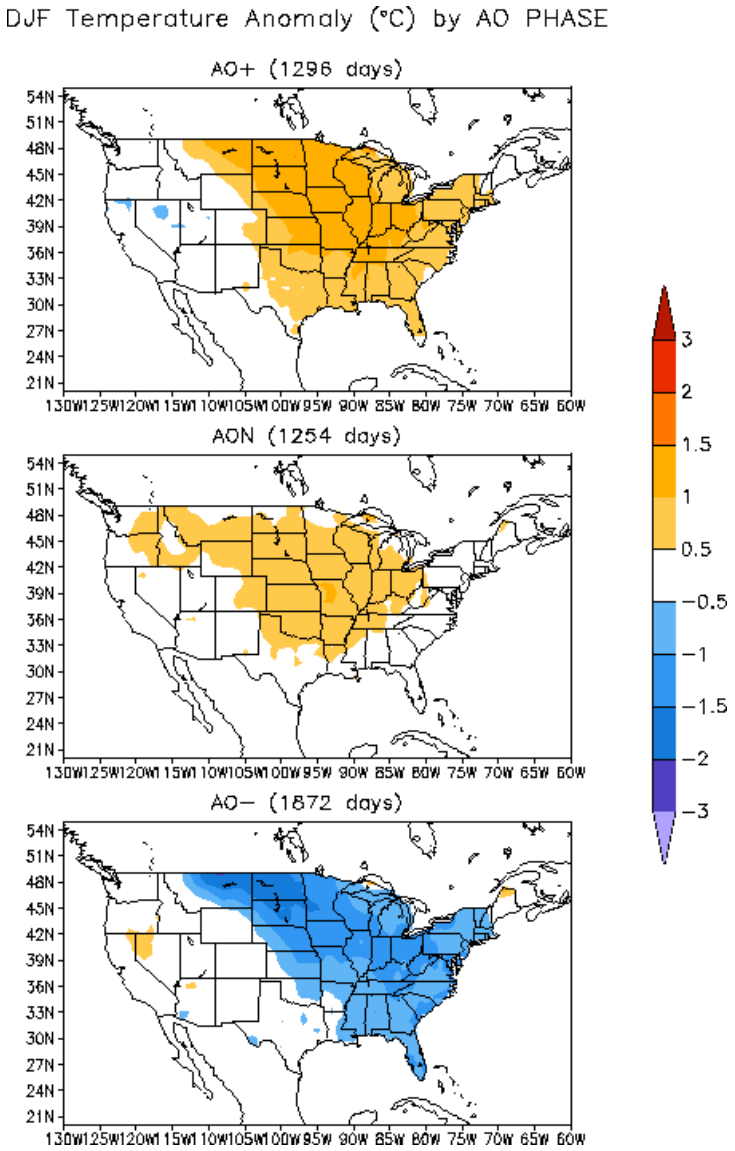


**Figure 11b.** Temperature anomalies (°C) in the continental United States during +AO (top), Neutral AO (middle), and –AO (bottom). During the negative state of the AO there are at least -1 °C temperature anomalies in the northeast United States, whereas during +AO the opposite is true.

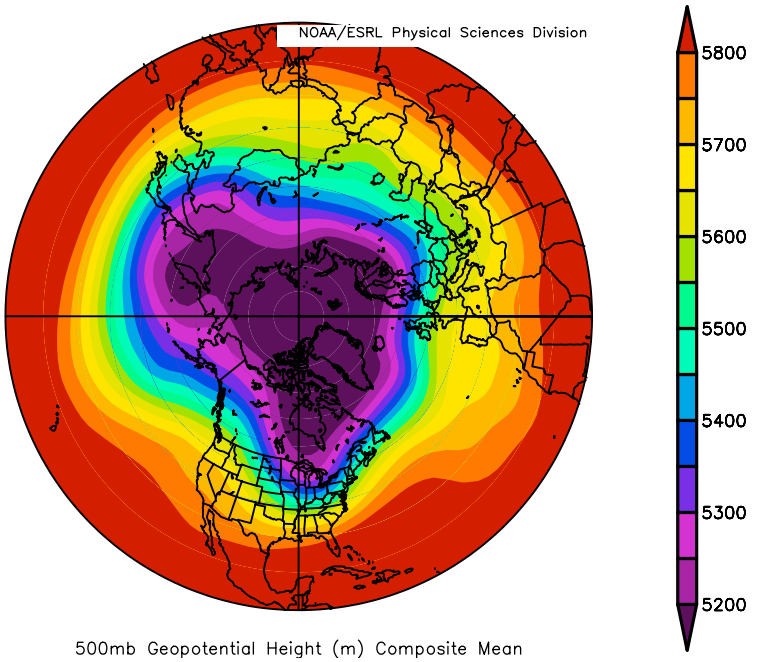


**Figure 12a.** Composite mean of the 500 hPa height (m) at onset for the cases the occurred during +AO.

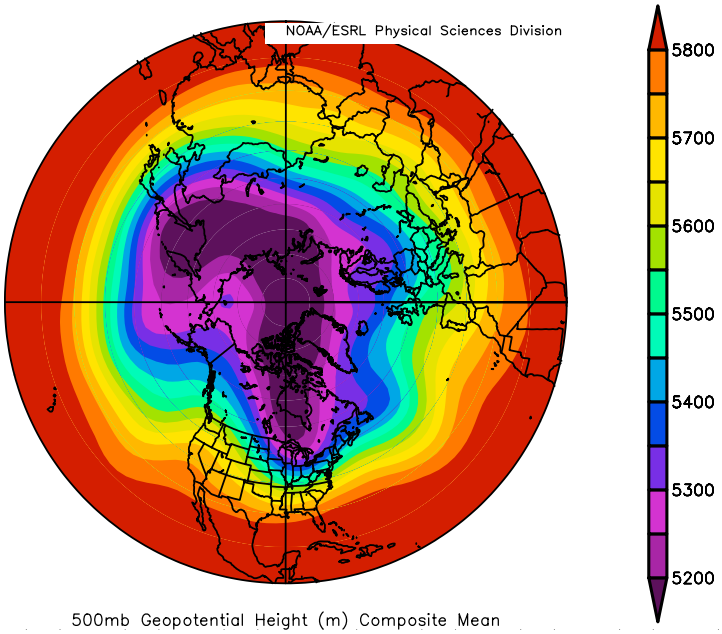


**Figure 12b.** As in 12a but for -AO.

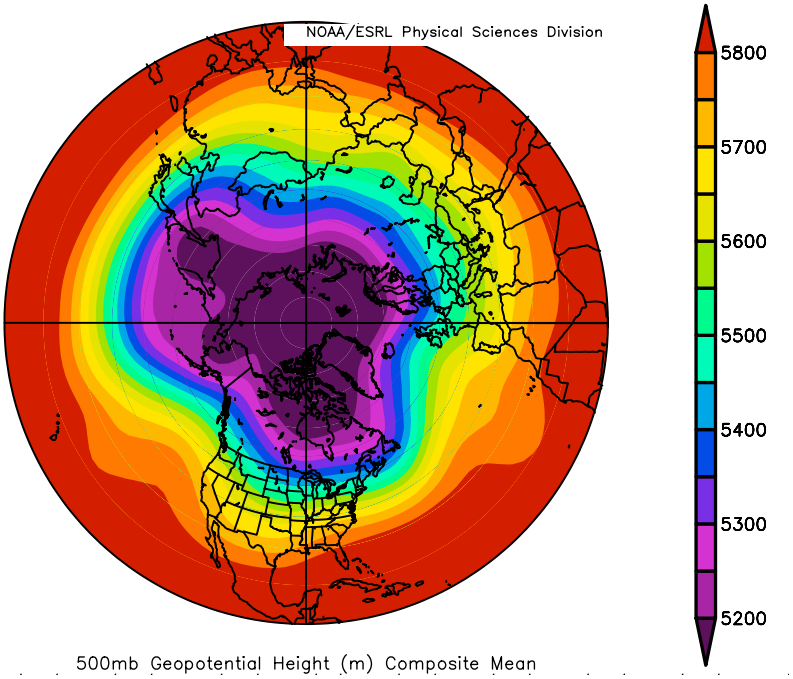


**Figure 13a.** Composite mean 500 hPa height (m) 3 days prior to onset for cases that occurred during +AO.

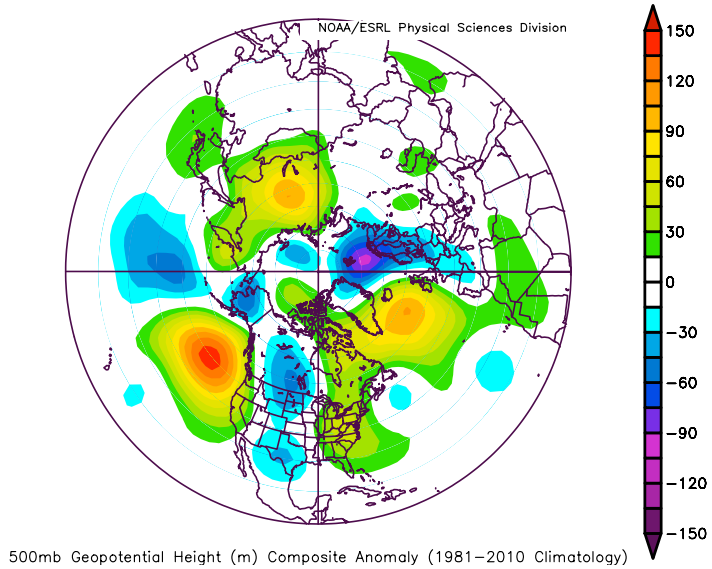


**Figure 13b.** As in 13a but anomaly values (m).

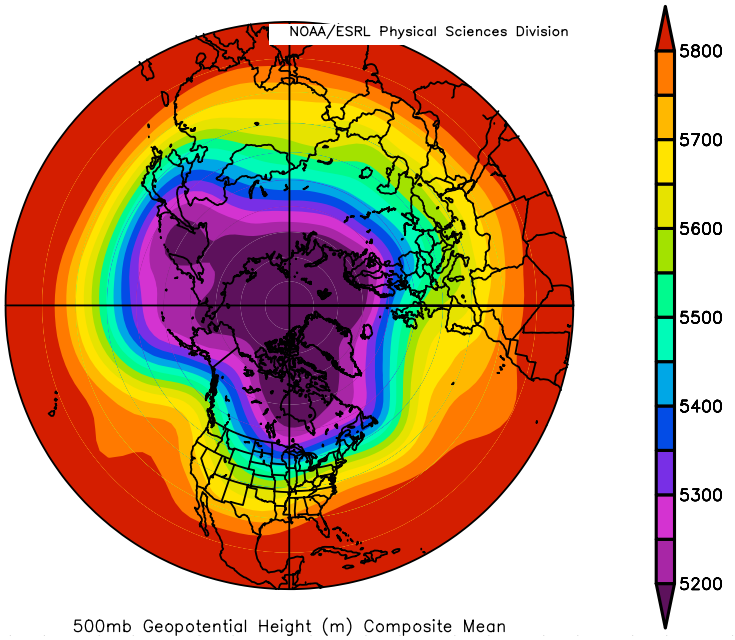


**Figure 13c.** As in 13a but 2 days prior to onset.

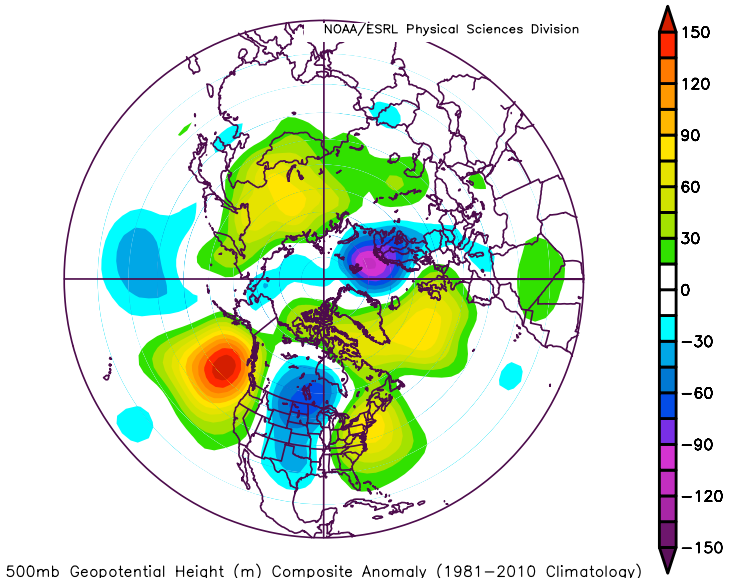


**Figure 13d.** As in 31c but the anomaly values (m).

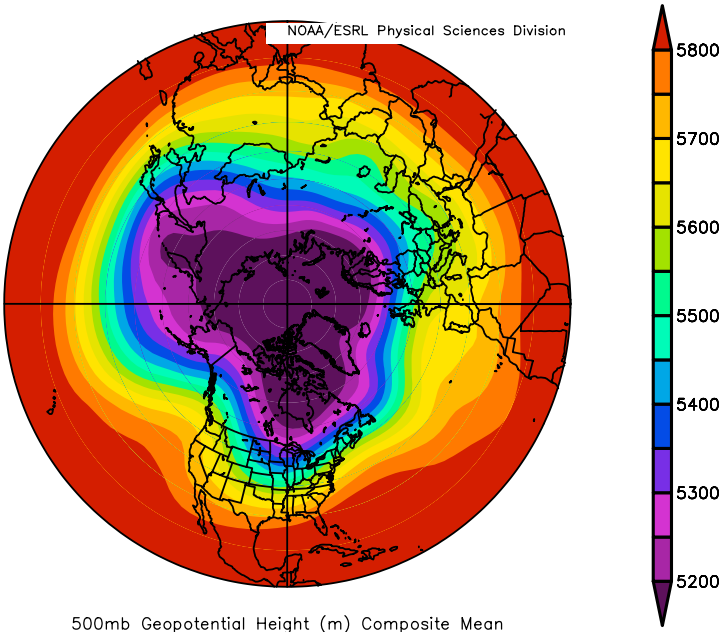


**Figure 13e.** As in 13a but 1 day prior to onset.

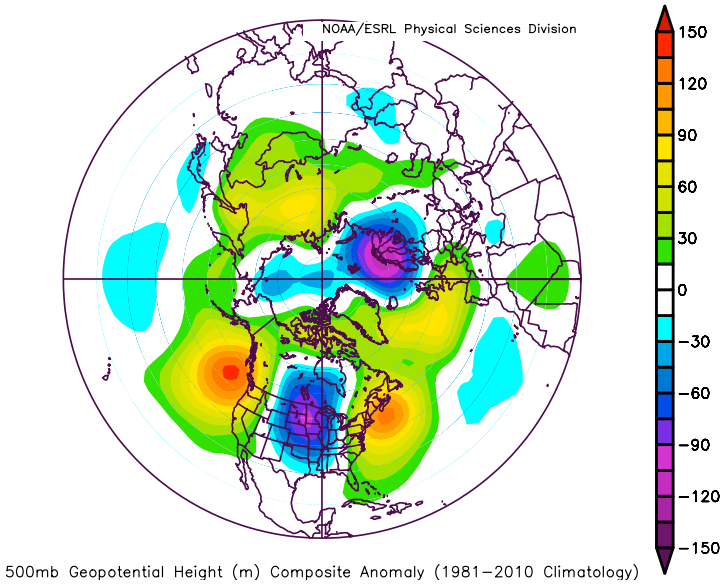


**Figure 13f.** As in 13e but anomaly values (m).

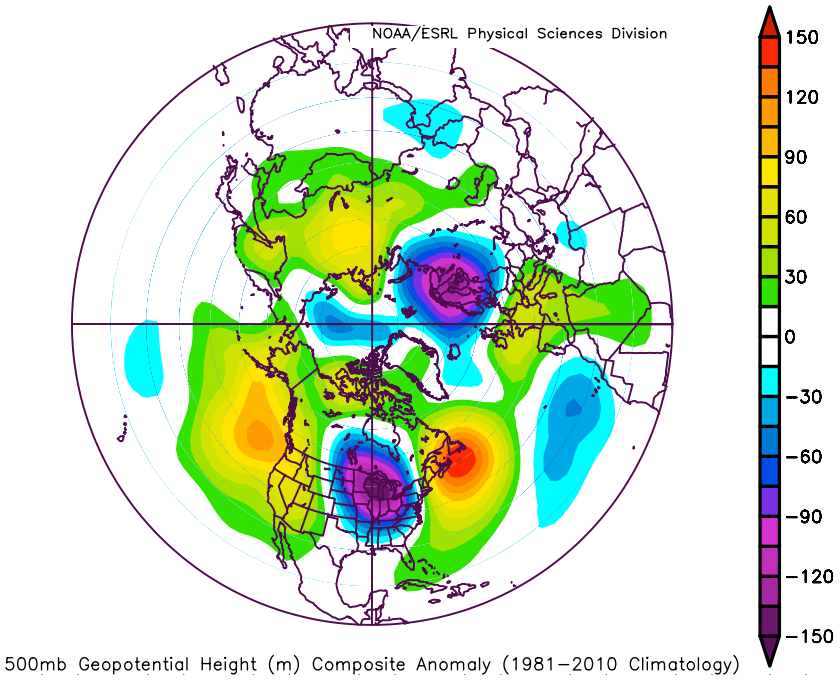


**Figure 13g.** 500 hPa height anomalies (m) at onset prior to onset for cases that occurred during +AO.

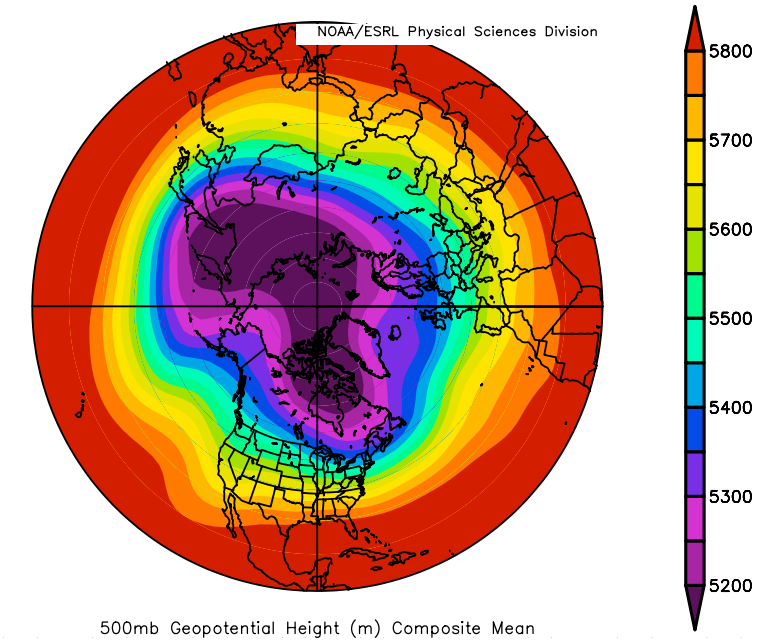


**Figure 14a.** Composite mean 500 hPa height (m) 3 days prior to onset for cases that occurred during -AO.

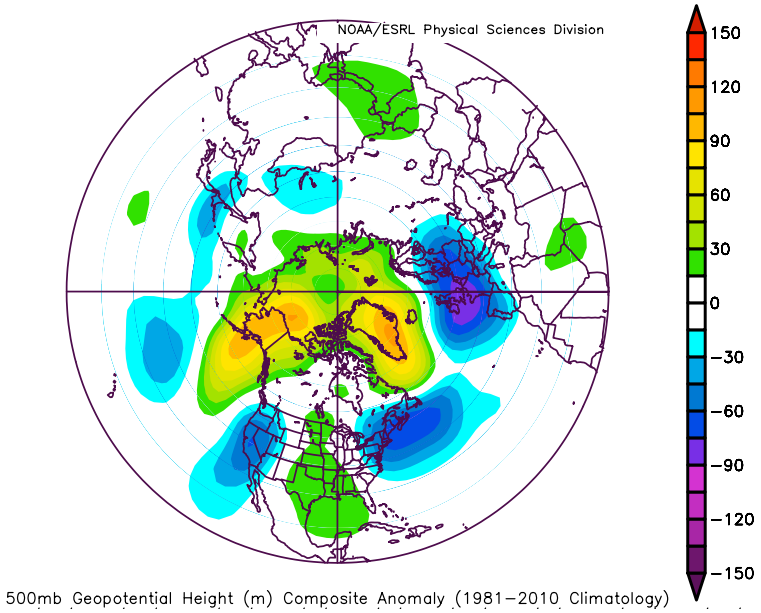


**Figure 14b.** As in 14a but anomaly values (m).

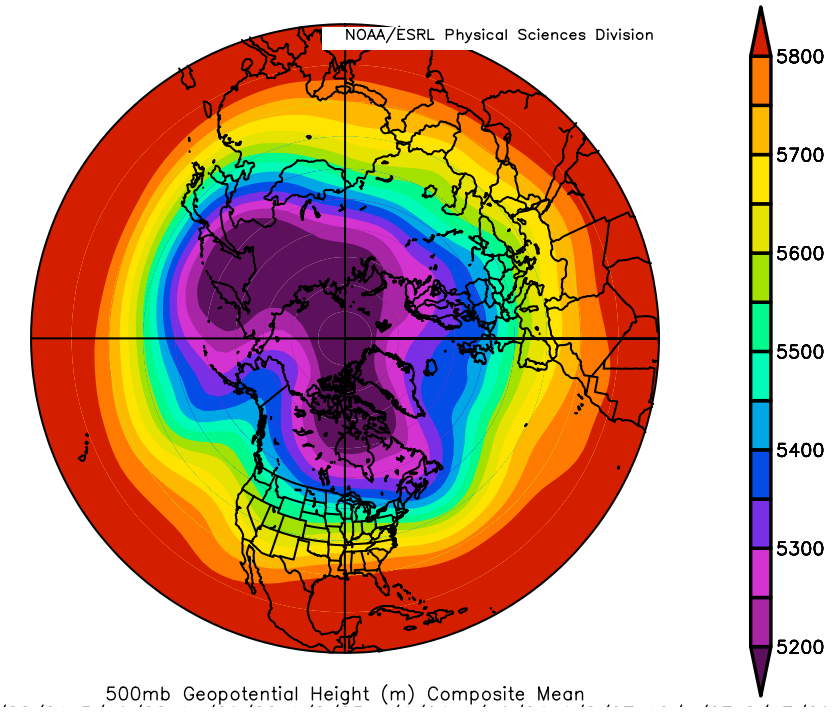


**Figure 14c.** As in 14a but 2 days prior to onset.

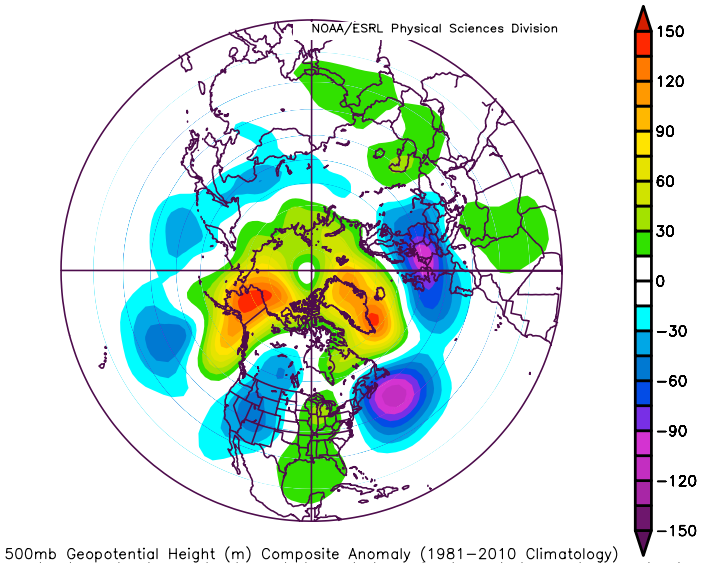


**Figure 14d.** As in 14c but anomaly values.

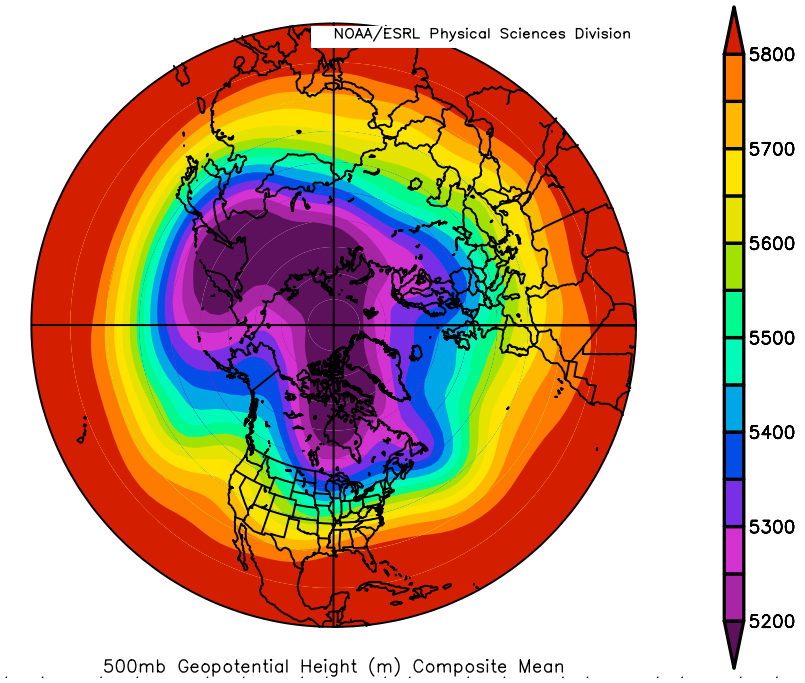


**Figure 14e.** As in 14a but 1 day prior to onset.

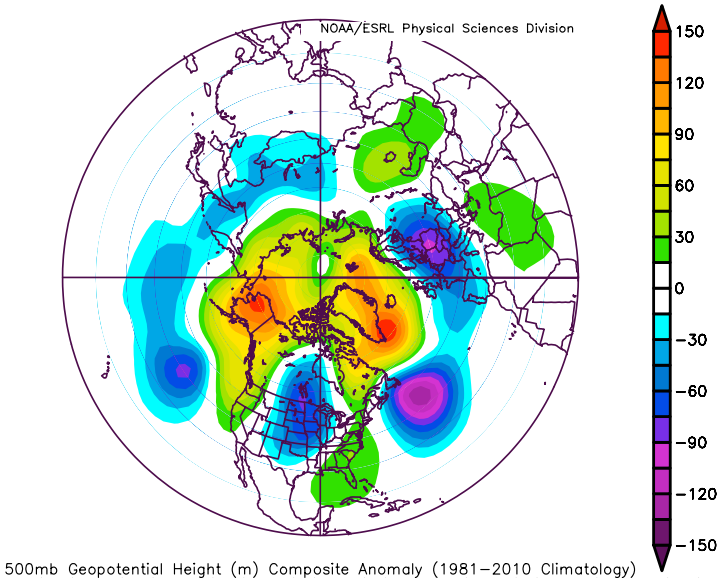


**Figure 14f.** As in 14e but anomaly values.

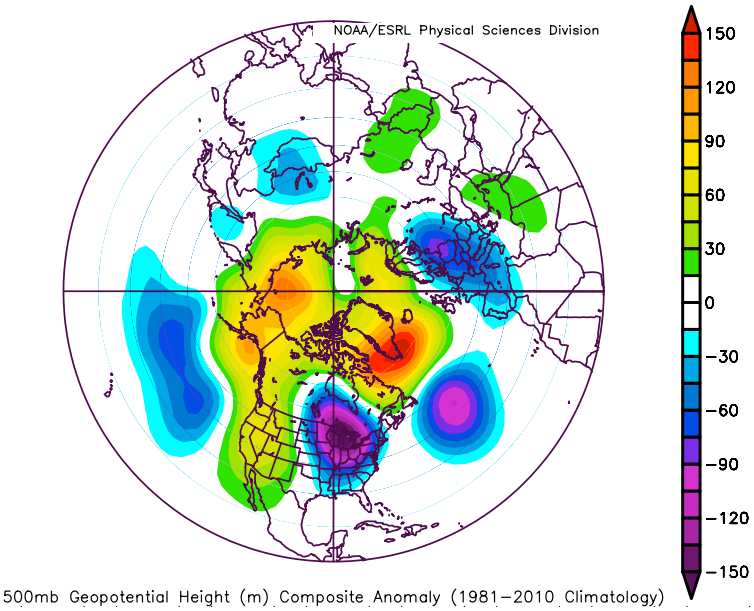


**Figure 14g.** 500 hPa height anomalies (m) at onset for cases that occurred during -AO.